◆ Human Brain Mapping 30:1568–1579 (2009) ◆

Movement Gating of Beta/Gamma Oscillations Involved in the N30 Somatosensory Evoked Potential

Ana Maria Cebolla,[1] Caty De Saedeleer,[1] Ana Bengoetxea,[1] Françoise Leurs,[1] Costantino Balestra,[2] Pablo d'Alcantara,[1] Ernesto Palmero-Soler,[1] Bernard Dan,[3] and Guy Cheron[1,4]*

[1]*Laboratory of Neurophysiology and Movement Biomechanics, Université Libre de Bruxelles, Brussels, Belgium*
[2]*Environmental and Occupational Physiology Laboratory, Haute Ecole Paul Henri Spaak, Brussels, Belgium*
[3]*Department of Neurology, Hopital Universitaire des Enfants reine Fabiola, Université Libre de Bruxelles, Belgium*
[4]*Laboratory of Electrophysiology, Université de Mons-Hainaut, Belgium*

Abstract: Evoked potential modulation allows the study of dynamic brain processing. The mechanism of movement gating of the frontal N30 component of somatosensory evoked potentials (SEP) produced by the stimulation of the median nerve at wrist remains to be elucidated. At rest, a power enhancement and a significant phase-locking of the electroencephalographic (EEG) oscillation in the beta/gamma range (25–35 Hz) are related to the emergence of the N30. The latter was also perfectly identified in presence of pure phase-locking situation. Here, we investigated the contribution of these rhythmic activities to the specific gating of the N30 component during movement. We demonstrated that concomitant execution of finger movement of the stimulated hand impinges such temporal concentration of the ongoing beta/gamma EEG oscillations and abolishes the N30 component throughout their large topographical extent on the scalp. This also proves that the phase-locking phenomenon is one of the main actors for the N30 generation. These findings could be explained by the involvement of neuronal populations of the sensorimotor cortex and other related areas, which are unable to respond to the phasic sensory activation and to phase-lock their firing discharges to the external sensory input during the movement. This new insight into the contribution of phase-locked oscillation in the emergence of the N30 and in its gating behavior calls for a reappraisal of fundamental and clinical interpretation of the frontal N30 component. *Hum Brain Mapp 30:1568–1579, 2009.* **© 2008 Wiley-Liss, Inc.**

Key words: evoked potential; somatosensorysystem; beta gamma oscillation; N30 component; phase locking

Contract grant sponsor: European Space Agency; Contract grant number: AO-2004, 118; Contract grant sponsors: Belgian Federal Science Policy Office; Belgian National Fund for Scientific Research (FNRS); Research Funds of the Université Libre de Bruxelles and of the Université de Mons-Hainaut (Belgium); PRODEX Fellowship (to AMC).

*Correspondence to: Prof. Guy Cheron, Laboratory of Neurophysiology and Movement Biomechanics, Université Libre de Bruxelles, CP 640, 50 Av F Roosevelt, Brussels, Belgium.
E-mail: gcheron@ulb.ac.be

Received for publication 20 December 2007; Revised 11 April 2008; Accepted 15 May 2008
DOI: 10.1002/hbm.20624
Published online 25 July 2008 in Wiley InterScience (www.interscience.wiley.com).

INTRODUCTION

Dynamic gating is a key aspect of neural processing allowing to select and enhance integration of stimuli and events that are most relevant to keep the focus on specific goals in the face of numerous environmental distractions [O'Reilly, 2006]. For example, it was recently demonstrated that sensory integration during reaching movement is a dynamic process driven by the task computational demands [Sober and Sabes, 2005]. It is generally accepted that gating mechanisms involve multiple parallel circuits including loops between the cortex, the basal ganglia, and the thalamus. Disinhibition and dopamine modulation play central roles in these neural networks [Durstewitz et al., 2000].

A possible way for noninvasive investigation of these processes in human resides in the analysis of the spectral content of neuronal oscillatory activity recorded in electroencephalographic (EEG) signals. This provides brain-state measure reflecting thalamo-cortical and cortico-cortical functioning [Buzsáki and Draguhn, 2004; Steriade, 2001]. As subcortical nuclei such as the thalamus are involved in the active gating of different sensory influx [Steriade et al., 1997] and contribute to change in EEG rhythms, the electrical median nerve stimulation provides a convenient and easily quantified sensory input for the study of the gating process.

Recent technological advances allow concomitant analysis of spontaneous ongoing EEG activity and evoked potentials [Delorme and Makeig, 2004; Makeig et al., 2002; Saunseng et al., 2007]. Relevant measures include the quantification of power changes in different frequency bands of the EEG signals with respect to stimulation. Among them, event-related spectral perturbation (ERSP) measure corresponds either to a narrow-band of event-related synchronization (power increase) or desynchronization (power decrease) of ongoing EEG activity. Another relevant measurement evaluates the level of phase-locking in different frequency bands of the ongoing EEG with respect to stimulation. This phase-locking factor [Tallon-Baudry et al., 1996] is here quantified by an intertrial coherence (ITC) measure. ERSP and ITC thus reflect physiological modifications of neural activity induced by external stimulation. This approach has led to a more comprehensive understanding of the origin of evoked potentials [Makeig et al., 2002; Sauseng et al., 2007 for a review].

The frontal or precentral N30 component of somatosensory evoked potentials (SEP) is known to be highly sensitive to interference or gating from concomitant involvement of the brain in sensory, motor, and mental activities [Cheron and Borenstein, 1987, 1991, 1992; Rossini et al., 1999; Rushton et al., 1981]. The amplitude of the frontal N30 significantly decreases when the stimulated hand performs an actual movement or during movement imagery [Cheron and Borenstein, 1991, 1992; Cheron et al., 2000]. Conversely, the observation of the same motor act by the subject at rest increases N30 amplitude [Rossi et al., 2002]. This wave is specifically modulated by electrical stimulation of the internal part of the globus pallidus or the subthalamus nuclei of Parkinsonian patients [Pierantozzi et al., 1999], suggesting that it may represent a reliable physiological index of the dopaminergic motor pathways [Cheron et al., 1994; Cheron, 1999]. Investigation of the frontal N30 component has increasingly been used in a host of clinical conditions [Fukuda et al., 2003; Murase et al., 2000; Pierantozzi et al., 1999; Tinazzi et al., 2004].

Recently, we have demonstrated that the N30 SEP component was accompanied by an increase of the power spectrum of beta/gamma rhythm peaking at 30 Hz and by a concomitant increase of the intertrials coherence at this frequency band [Cheron et al., 2007]. Pure phase-locking of the beta/gamma rhythm was found in a large percentage of the trials. We also demonstrated that a reorganization of the spontaneous phase of the ongoing beta rhythm contributed to the production of N30 component.

Here, we investigated the behavior of this pure phase-locking during the gating produced by movement of the stimulated hand. A major hypothesis of the present study is that the decrement in N30 amplitude during movement gating was mainly due to an alteration in the beta/gamma phase-locking mechanism.

METHODS

Subjects and Conditions

The data were collected from 14 normal volunteers (seven females and seven males, mean age: 26 ± 3.2 years). They were in good health and free from neurological disease. The procedures were approved by the local ethics committee of the University and conformed to the Declaration of Helsinki.

Somatosensory evoked potentials (SEP) were recorded at rest with the eyes closed and during a movement interference task. During this task the subjects were asked to flex and extend four fingers of the stimulated hand (not the thumb) together. Finger movements were unrelated to the stimulation.

SEP Stimulation and Recording Parameters

The stimuli were 0.2 ms square electrical pulses delivered through a pair of Ag–AgCl electrodes cup to the left median nerve at the wrist. The intensity was adjusted for eliciting visible small thumb twitches. Random stimuli intervals (0.5–2 s range) were used throughout the experiment. In the first group of seven subjects, the standard electrode positions corresponded to F3, F4, a contralateral, and an ipsilateral parietal site situated 70 mm from the midline and 30 mm behind C4–C3 [these loci correspond to the site where the N20 component was maximally recorded when the contralateral wrist was stimulated [Desmedt and Cheron, 1980]; all electrodes were referred to the contralateral earlobe. The on-line SEP averaging was performed using a four-channel NihonKohden averager (Neuropack, MEB-9100). The overall band-pass was 0.5

Hz–1.5 kHz and the analysis time was 100 ms with a sampling rate of 5 kHz. Scalp electrodes impedances were kept below 5 kΩ. Two series of 500 potentials were checked for reproducibility. After ocular artefact reduction, any remaining artefacts were rejected by visual inspection. As the averager used does not permit the spectral analysis of the single sweep data and to independently analyze the ongoing rhythmic EEG activity from the evoked response, the raw (unaveraged) EEG data were transferred in parallel to a Pentium III personal computer with analog-to-digital converter boards (Digidata Axoscope). This analysis was only performed on the F4 channel. Off-line analysis and illustrations were then performed using the EEGLAB software [Delorme and Makeig, 2004].

To perform topographical analysis of SEP gating, SEPs were recorded using 128 channels EEG recorder (ANT system, The Netherlands) in a second group of seven subjects. This system uses full-band DC amplifier including active-noise cancellation process, worked at a sampling frequency of 2,048 Hz, and with a resolution of 22 bit (71.5 nV per bit). An active-shield cap using 128 Ag–AgCl sintered ring electrodes and shielded coaxial cables (5–10 electrode system placement) was comfortably adjusted to subject head.

Event-Related Spectral Perturbation

The EEGLAB software enables the analysis of the event-related average dynamics changes in amplitude of the broad band EEG frequency spectrum and to decipher the ongoing EEG processes that may be partially time- and phase-locked to experimental events [Delorme and Makeig, 2004]. The event-related spectral perturbation measure (ERSP) may correspond to a narrow-band of event-related desynchronization (ERD) or synchronization (ERS). Briefly, for this calculation, EEGLAB computes the power spectrum over a sliding latency window on each epoch and normalizes each of them by its respective mean baseline spectra and then performs averaging across data trials. Each trial consists of samples from −400 ms before up to 400 ms after the stimulus. The size of the sliding window was of 512 data points. ERSP image provides a color code where each template pixel indicates the power (in dB) at a preset frequency f and latency t relative to the stimulation onset. Typically, for n trials, if $F_k(f, t)$ is the spectral estimate of trial k at frequency f and time t,

$$\mathrm{ERSP}(f,t) = \frac{1}{n}\sum_{k-1}^{n} \left|F_k(f,t)\right|^2 \tag{1}$$

To compute $F_k(f, t)$, EEGLAB uses the short-time Fourier transform that provides a fixed time and frequency resolution.

Intertrial Coherence

Intertrial coherence (ITC) is a frequency-domain measure of the partial or exact synchronization of activity at a particular latency and frequency to a set of experimental events to which EEG data trials are time-locked. This measure corresponds to the "phase-locking factor" [Tallon-Baudry et al., 1996]. The term ITC refers here to its interpretation as the event-related phase coherence (ITPC), which is defined by

$$\mathrm{ITPC}(f,t) = \left|\frac{1}{n}\sum_{k-1}^{n} \frac{F_k(f,t)}{\left|F_k(f,t)\right|}\right| \tag{2}$$

where $|\cdot|$ represents the complex norm. The ITC measure takes values between 0 and 1. A value of 0 represents absence of synchronization between EEG data and the time-locking events; a value of 1 indicates their perfect synchronization.

The significance levels of the ITC and ERSP were fixed at 0.001 and assessed using surrogate data by randomly shuffling the single-trial spectral estimates from different latency windows during the baseline period (EEGlab bootstrap method).

Selection of Trials With Pure Phase Resetting

The single sweep selection aims to conserve only the trials for which the EEG amplitude of the filtered signal (e.g. 25–35 Hz) measured around the N30 latency remained similar compared to the prestimulus amplitude. For this, we compared in each filtered single-sweep the root-mean-square (RMS) amplitude of the pre- and post-stimulus periods ([−200, 0 ms] and [0, +60 ms], respectively) according to the following equation:

$$\Delta\mathrm{RMS} = \frac{(\mathrm{RMS}_{\mathrm{post}} - \mathrm{RMS}_{\mathrm{pre}})}{(\mathrm{Max\ Ampl})} \tag{3}$$

where Max Ampl, the maximal amplitude of the filtered single sweep signal, is measured for the period ([−200, 0 ms]). Then, we selected only the trials for which the following criterion was respected:

$$\Delta\overline{\mathrm{RMS}}_{\mathrm{stim-free}} - 1\mathrm{SD} \le \Delta\mathrm{RMS}_{\mathrm{data}} \le \Delta\overline{\mathrm{RMS}}_{\mathrm{stim-free}} + 1\mathrm{SD} \tag{4}$$

where $\Delta\mathrm{RMS}_{\mathrm{data}}$ was compared to $\Delta\mathrm{RMS}_{\mathrm{stim\text{-}free}}$ for two periods free of stimulus ([−350, −150 ms] and [−150, −90 ms]). After that, it was verified that the selected $\Delta\mathrm{RMS}_{\mathrm{data}}$ distribution was included inside the $\Delta\mathrm{RMS}_{\mathrm{stim\text{-}free}}$ distribution. This means that no significant amplitude enhancement or decrement were present in these selected trials.

Phase Histogram Analysis

The degree of synchronization of the ongoing EEG oscillation was assessed by means of histograms of the instantaneous phase of the components across an ensemble of the selected trials [Jansen et al., 2003]. Phase histograms of the components found in the beta (25–35 Hz) band in the

selected trials were generated every 5 ms, starting 60 ms before stimulus up to 150 ms after stimulus. The Kuiper statistic κ coefficient, expressed as a ln, was used to evaluate differences in empirical distribution functions [Press et al., 1992] and to quantify the degree with which the phase histograms resembled a uniform density function. κ is defined as

$$\kappa = \ln\left\langle 2\sum_{j=1}^{\infty}(4j^2V^2 - 1)e^{-2j^2V^2}\right\rangle, \quad (5)$$

with

$$V = \left(\sqrt{N} + 0.155 + \frac{0.24}{\sqrt{N}}\right) \times \left[\max_{i=1,\ldots,L}[S_N(x_i) - F_0(x_i)] + \max_{i=1,\ldots,L}[F_0(x_i) - S_N(x_i)]\right], \quad (6)$$

where $F_0(x_i)$ and $S_N(x_i)$ are the mean pre-stimulus reference period [−60, −5 ms] and the actually observed cumulative distribution function, respectively; N is the effective number of data points, L the number of bins in the histogram and x_i the upper bound of bin i.

The more the observed $S_N(x_i)$ is different from the reference $F_0(x_i)$, the more κ will be negative. Z-score of κ was used to provide further evidence of reliability of the effect across subjects. As the Z scores are defined through individual subject mean and SD, it results in different statistical levels at rest and during movement gating.

Data were analyzed using a one-way ANOVA test and Bonferroni's post-hoc test after assessing their normality by a Kolmogorov–Smirnov test (Statistica 7.1, Statsoft). Differences were considered significant at $P < 0.05$. Results are expressed as means ± SD.

RESULTS

To highlight the extent of movement gating on the frontal N30 component, we performed topographical studies by mean of a 128 channels recording (ANT system) in seven subjects. Figure 1 illustrates topographical differences for each subject, at rest (Fig. 1A) and during movement gating (Fig. 1B). Response amplitude changes between both conditions were compared by means of MANOVA test ($P \leq 0.05$) for the 128 channels in the seven subjects (Fig. 1C).

At rest, the negativity at 30 ms spreads mainly on the whole frontal and central areas with more extension toward ipsilateral parietal area, as classically described. A concomitant positivity was present on the contralateral parietal area. During movement gating, the frontal negativity is significantly decreased on the whole extent of the frontal and central areas (Fig. 1C).

ERSP and ITC Analysis in Grand Averaged Data

Figure 2 illustrates the movement gating in a grand average display representing the relationship between the

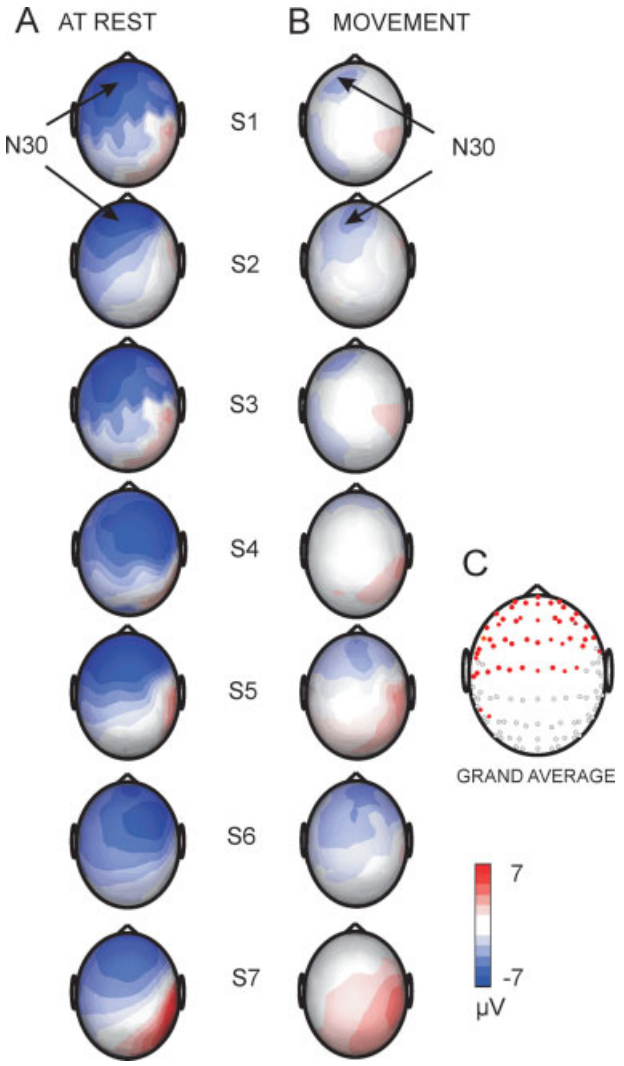

Figure 1.
Topographical extent of the movement gating of the N30 component. Potential scalp distribution for seven subjects with 128 channels, at rest (**A**) and during gating (**B**) of the N30 component. (**C**) Response amplitude changes between both conditions calculated by MANOVA test ($P \leq 0.05$) on the 128 channels for the seven subjects: red circles represent electrodes with significant values of change in amplitude. [Color figure can be viewed in the online issue, which is available at www.interscience.wiley.com.]

frontal N30 component and the related ERSP and ITC at rest (Fig. 2A–C) (3,000 trials, $n = 7$ subjects, F4 channel, NihonKhoden system) and during the movement gating (Fig. 2D–F) (3,039 trials, $n = 7$ subjects). At rest, a significant phase-locking in the beta/gamma band oscillation (mean frequency: 33.1 ± 1.3 Hz) peaking at a latency of 34.9 ± 5.2 ms and expressed by a maximal ITC value of 0.53 ± 0.17 is accompanied by an ERSP cluster (peaking at 35.2 ± 6.3 ms) with a maximal value of 2.4 ± 1.5 dB. Concerning alpha rhythm, cluster with smaller ITC maximal

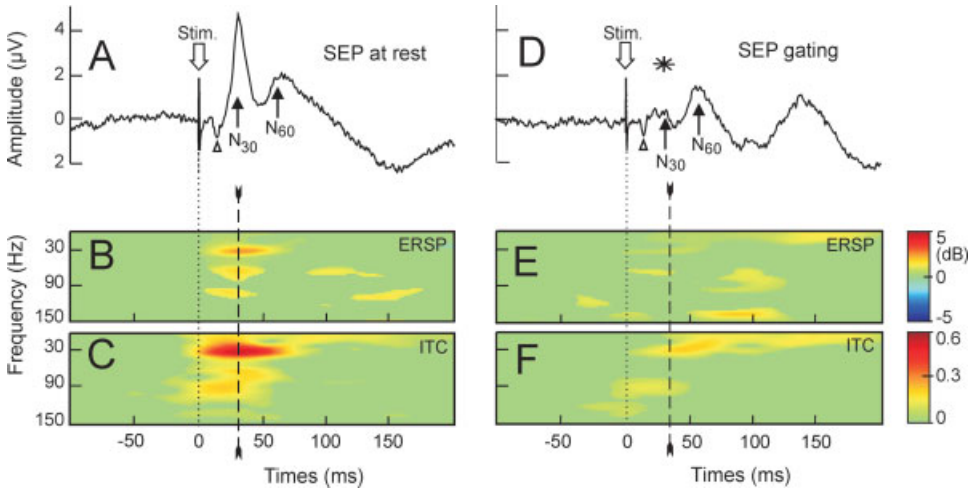

Figure 2.

Grand average analysis of N30 component at rest and during movement gating. (**A**, **D**) Grand average of the frontal N30 component recorded from F4 during median nerve stimulation at the wrist at rest and during movement gating conditions, respectively. Little open triangle peaking at P14. (**B**, **C**, **E**, **F**) Grand average of time/frequency template from ERSP and ITC analysis, for both conditions. Note that the peak of ERSP and ITC value in the beta range (25–35 Hz) coincided with the N30 latency peak at rest. [Color figure can be viewed in the online issue, which is available at www.interscience.wiley.com.]

value (0.29 ± 0.10) at the latency of 54.8 ± 40.5 ms was not accompanied by significant ERSP cluster value. Faster rhythms than 30 Hz were not systematically present in all the subjects; there are not on the scope of the present study.

The conservation of the same amount of the afferent drive during the movement gating was demonstrated by the absence of significant modification of the amplitude of the subcortical P14 far-field (1.1 ± 0.5 μV at rest vs. 0.84 ± 0.5 μV during movement, $P = 0.34$) and of the parietal N20 component reflecting the first cortical activation (1.8 ± 0.7 μV at rest vs. 1.7 ± 0.6 μV during movement). The main effect of the movement gating was a very strong reduction in N30 amplitude [4.8.± 1.8 μV at rest (Fig. 2A), vs. 0.7 ± 0.5 μV during the movement gating (Fig. 2D)], while the amplitude of the following N60 component remained unchanged. The gating of the N30 amplitude was accompanied by a significant reduction of the ITC cluster value at 30 Hz (0.53 ± 0.17 at rest vs. 0.26 ± 0.07 during movement $P < 0.001$) (Fig. 2F). In this condition, the diffuse alpha ITC cluster and the beta/gamma ITC cluster were also shifted toward longer latency (112.0 ± 35.3 ms and 56.2 ± 14.6 ms for alpha and beta/gamma and rhythms, respectively). The ERSP plot also showed the disappearance of beta ERSP cluster for all the poststimulus period analyzed (Fig. 2E). This disorganization of the beta/gamma oscillation phase-locking by the movement gating is illustrated by the comparison of the superimposition of the filtered (25–35 Hz) EEG trials at rest (Fig. 3A) and during the gating movement (Fig. 3B). At rest, spontaneous beta oscillations were reorganized in relation to the stimulus. In this case, the negative part of single beta oscillation peaked at the latency of the N30 component. Conversely, during the movement gating such temporal reorganization was absent and beta waves were not phase-locked to the median nerve stimulation.

As identification of phase resetting of spontaneous EEG activities in certain frequency bands requires the demonstration of the presence of these EEG oscillations in the absence of stimulus, we measured the power spectrum of the spontaneous beta oscillation in each single trial excluding the periods of evoked activity both in rest and movement conditions. For all the recorded trials, the mean of the beta/gamma power spectrum represented a value of 17.1 ± 4.9 dB at rest and 17.2 ± 2.5 during movement gating. For comparison, the mean power spectrum of the dominant α-mu rhythm (~10 Hz) during the same period was 26.4 ± 5.3 dB at rest and 26.5 ± 3.3 during movement gating. This suggests that the beta/gamma oscillation (representing about 65% of the alpha rhythm power both at rest and during movement gating) may be involved in a phase-locking process in both conditions.

As it was demonstrated that in case of *phase-locking with enhancement*, which corresponds to the present situation at rest, it was impossible to distinguish the possible contribution of EEG phase-resetting from phasic activity [Shah et al., 2004; Yeung et al., 2004], we restricted our analysis on the trials of individual subjects for which the power spectrum remained unchanged after the stimulation.

For each of the seven subjects, we identified at rest a large percentage of trials (62 ± 16%) for which the power spectrum remained unchanged (pure phase-locking situation) within the whole frequency range spanning 1–50 Hz. Figure 4 illustrates results of this selection in one subject.

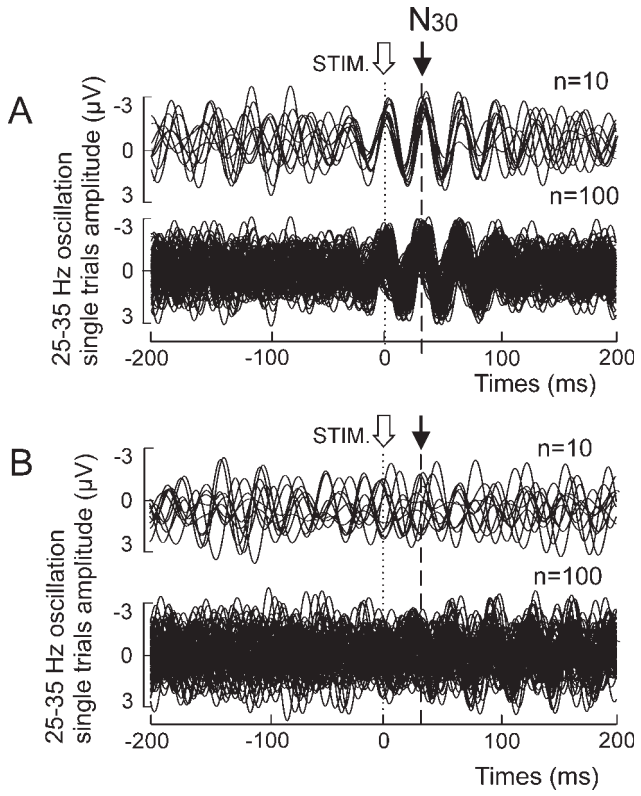

Figure 3.

Superimposition of single-filtered (25–35 Hz) EEG trials with respect to median nerve stimulation at rest (**A**) and during movement gating (**B**). For each condition, 10 (upper traces group) and 100 (lower traces group) trials are superimposed. Note that at rest the phase rearrangement involves concentration of negative wave at the latency of the N30 component.

When all the recorded trials were taken into account, a clear ERSP cluster appeared in the beta/gamma band (Fig. 4A) concomitantly accompanied by a significant ITC cluster in the same frequency band (Fig. 4B). After the selection, although no more ERSP cluster could be found (Fig. 4D), a significant ITC cluster in the beta/gamma band was still present (Fig. 4E). A decrease of power in a large frequency band occurred around 100 ms meaning that it may thus not participate in the N30 generation. The maximal ITC value (0.51 before vs. 0.55 after selection), peak latency (42 ms before vs. 41.4 ms after), and frequency band (19–44 Hz before vs. 23–44 Hz after) of the ITC cluster were not significantly changed by the trial selection (Fig. 4B–E). Conversely, the N30 amplitude was significantly reduced by the selection [mean amplitude of 4.5 ± 1.7 vs. 3.6 ± 1.2 μV, $P < 0.02$ (Fig. 4C, F)]. In spite of this amplitude reduction, the N30 component conserved its initial morphology and peaked at the same latency (mean value 31.3 ± 0.9 ms before selection vs. 31.1 ± 0.9 ms after). After the selection procedure the relative percentage of the 30 Hz power, in the period excluding the stimulation, remained the same (66.6%).

For comparison, the same subject is illustrated during the movement gating (Fig. 4G–I). In this case, no significant ERSP change was observed after the stimulation (Fig. 4G) and the pure phase-locking selection procedure was thus not necessary. During movement gating, the ITC cluster in the beta range around 30 ms was dramatically decreased and diluted (from 0.51 to 0.24 ITC max value).The ITC surface in the beta band is centered in this case at 68.5 ms (Fig. 4H). The mean latency of the beta/gamma ITC peak was 34.9 ± 5.2 ms at rest versus 56.25 ± 14.66 ms during the gating. As shown in the illustrated subject, this new ITC picture accompanied the important reduction of the N30 amplitude from 4.2 to 1.12 μV (Fig. 4I).

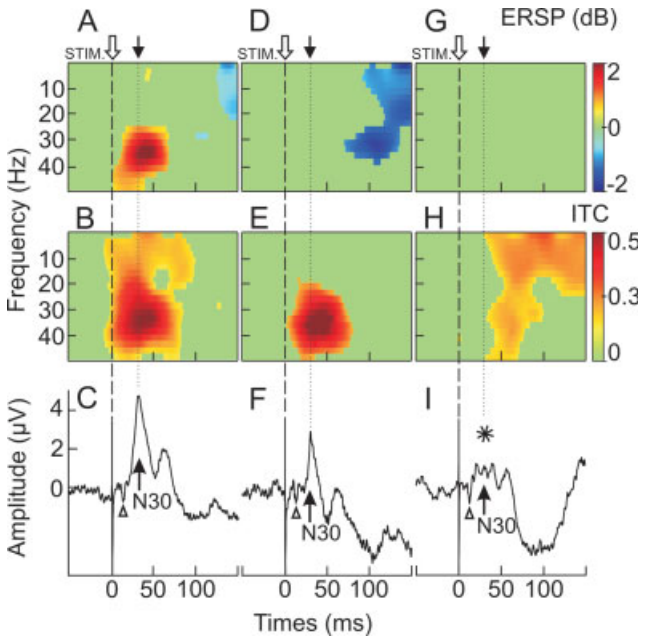

Figure 4.

Selection of pure phase-locking and movement gating effect illustrated for one subject. (**A**–**C**) ERSP, ITC, and N30 evoked potentials, respectively, recorded when all the trials were taken into account. Note that this situation corresponds to phase-locking with amplitude enhancement, where the N30 component was accompanied by significant ERSP (**A**) and ITC (**B**) cluster in the β-gamma frequency range. (**D**–**F**) ERSP, ITC, and N30 evoked potentials, respectively, recorded when only the trials for which no amplitude enhancement were taken into account. This situation corresponds to pure phase-locking where the N30 component was only accompanied by the ITC cluster in the β-gamma range. Note the reduction of the N30 amplitude in the pure phase-locking situation (**F**). (**G**–**I**) ERSP, ITC, and N30 evoked potentials, respectively, recorded during movement gating. Note the absence of ERSP and ITC clusters at the N30 latency and the major reduction of this evoked component. [Color figure can be viewed in the online issue, which is available at www.interscience.wiley.com.]

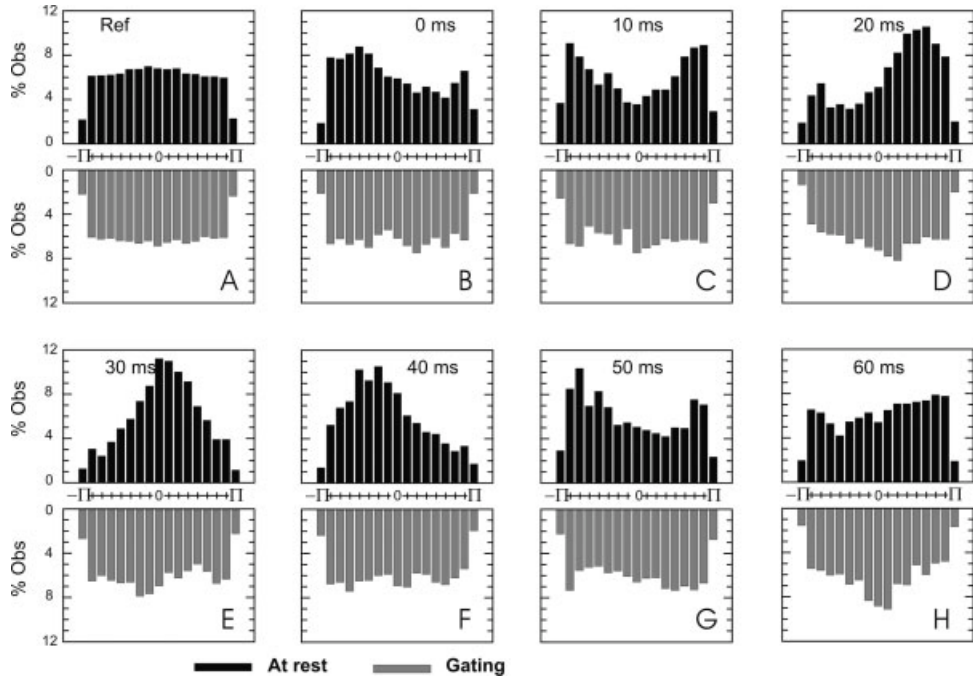

Figure 5.

Reorganization of the spontaneous phase of beta oscillation at rest and during movement gating. Cumulative histograms of the spontaneous phase of single trials beta band oscillation (25–35 Hz) recorded in all the subjects (pooled as a single set) and selected with respect to the pure phase-locking criteria. Upper black colored histograms and Lower gray colored histograms correspond, respectively, to the data recorded at rest and during the movement gating. Horizontal phase axis ranges from $-\pi$ to π. Vertical axis corresponds to the relative number of trials. (**A**) Histograms for the prestimulus reference period ([−60 ms, −5 ms]). (**B**–**H**) Histograms from 0 to 60 ms with respect to the stimulation time (illustrated at every 10 ms). Note the progressive reorganization of phase distribution peaking at 0 radian at 30 ms at rest and the absence of reorganization during the movement gating.

Phase-Locking Analysis

To compare the temporal reorganization of beta oscillations following median nerve stimulation in the resting and movement gating conditions, the instantaneous phase of each selected trial recorded in each condition was calculated along time for each subject. Figure 5 shows relative cumulative histograms of instantaneous phase of the selected trials of all the subjects at rest (n = 1,739) (upper part black colored histograms) and during gating (lower part grey colored histograms). Before the stimulus, both at rest and during gating condition, the histogram of phase distribution corresponds to uniform density function (Fig. 5A). In the resting condition, a phase alignment occurred after the stimulus and the phase distribution became gradually more peaked so that the distribution presents a maximum of trials with an instantaneous phase value of 0 radian at the latency of the N30 component (upper part of Fig. 5E). The comparison between the mean histogram calculated for the prestimulus reference period (Fig. 5A) and the 30 ms poststimulus time (Fig. 5E) showed a clear distinction between uniform and peaked distribution at 0 radian, in the resting condition. In contrast, during the movement gating, the phase distribution remained practically the same and no clear peaked distribution emerges at the latency of the N30 component.

Figure 6 illustrates in both resting and gating conditions the mean Z score of the Kuiper's statistic κ. The phase distribution difference between the prestimulus reference period ([−60 ms, −5 ms]) and the poststimulus times was significant ($P < 0.05$) below a Z score value of 0.68 and 0.047 for both conditions, respectively. In the resting condition, significant threshold was reached for each analyzed time after the stimulus and became highly significant around the N30 latency, reaching a value of -1.44 ± 0.28. In contrast, the mean Z score did not reach significant value around 30 ms during movement gating. The most significant Z score value (−0.85) in this condition corresponded to the least peaked distribution observed at 60 ms in Figure 5H.

DISCUSSION

Our findings demonstrate that the N30 component results from two different mechanisms. One is related to a

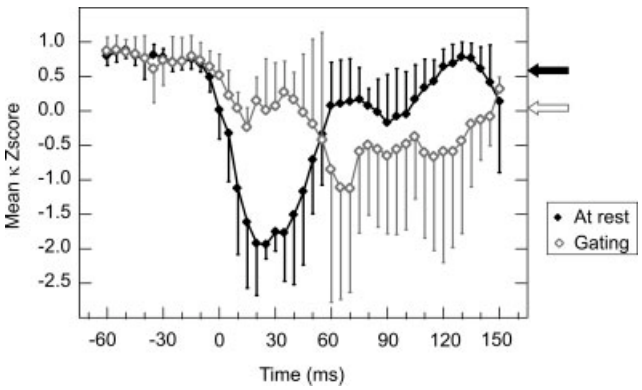

Figure 6.

Statistical analysis of the beta phase distribution at rest and during movement gating. Evolution of the *Z* score (mean and SD) of the Kuiper's statistic κ. *Z* score is significant ($P < 0.05$) below 0.68 and 0.047, and the highest significant values are reached around a poststimulus time of 30 and 60 ms, for the resting and gating conditions, respectively.

phasic process that produces by its inherent properties (stimulus locked) an evoked potential accompanied by a β-gamma power increase. The other is related to a pure phase-locking mechanism. As the gating produces a complete and specific suppression of both β-gamma ERSP increase and ITC occurring at the N30 latency, we may propose that the gating interference affects both the phasic and the oscillating generator mechanisms. Nevertheless, it is only when the ITC is suppressed that the N30 is gated. In this context, the relative functional independence of an oscillating generator mechanism with respect to a phasic generator mechanism plays in favor of a dual nature of the N30 component. This physiological characteristic may be supported by more than one single generator model. It is interesting to note that phase-locking phenomenon is often supported by long range neuronal synchronization implicating communication between distinct areas [Singer, 1999 for a review]. This could corroborate the findings of Kanovsky et al. [2003] describing separate generators within the frontal cortex (BA6 and BA8). These intracortical N30 recordings performed in epileptic patients also reproduced the gating protocols [Cheron and Borenstein, 1987, 1992]. In particular, the mental movement paradigm inducing a blood flow increase in the SMA (BA6) [Roland et al., 1980] produced a specific gating of the N30 without affecting the postcentral components [Cheron and Borenstein, 1992]. This N30 suppression was reproduced by intracortical SMA recordings [Kanovsky et al., 2003] indicating that this region at least could be a source of the N30 component. The current debate concerning the interpretation of the intracortical N30 recording comes from the difficulties to record polarity-reversal potentials in the frontal lobe [see Barba et al., 2001, 2003, 2005; Barba and Valeriani, 2004]. Taking into account the convolutional anatomic conformation of the cortex, the polarity-reversal recording may be highly difficult if not impossible. Nevertheless, in addition to the gating approach a large set of evidence has been accumulated in favor of a frontal origin of the N30, namely (1) the N30 amplitude depends on motor cortex excitability [Rossini et al., 1991], (2) apomorphine injection or electrical stimulation of the basal ganglia induced selective increase of N30 amplitude in Parkinsonian patients [Cheron et al., 1994; Pierantozzi et al., 1999; Rossini et al., 1995], (3) transcranial magnetic stimulation (TMS) of the premotor cortex at very low frequency rate produced a specific N30 amplitude increase [Urushihara et al., 2006]. These latter authors hypothesized that this effect may be due to an increase in premotor cortex inhibition. As we demonstrate here that N30 is supported by β-gamma oscillation, the inhibition-timing hypothesis [Klimesch et al., 2007] may explain a N30 amplitude increase in presence of increasing inhibition produced by TMS and conversely a N30 decrease in presence of increasing excitation of premotor and motor areas produced by movement execution.

Although, gating during active movement may be due to a combination of both central and peripheral factors, in agreement with earlier gating studies [Cheron and Borenstein, 1987, 1991; Cohen and Starr, 1987; Jones et al., 1989], the present study showed no gating of the SEP wave at subcortical levels below the thalamus [indexed by the conservation of the far-field P14, originating in the median lemniscus [Desmedt and Cheron, 1981] and between the thalamus and the first parietal activation [indexed by the conservation of the parietal N20, generated by a tangentially oriented dipole located in area 3b of the posterior bank of the central sulcus [Allison et al., 1989]. However, there are some controversies concerning the gating of the parietal N20. A small but significant decrease has been found during vibration interference [Ibanez et al., 1989], passive and active movements [Huttunen and Hömberg, 1991]. A similar N20 gating has been described by Gobbelé et al. [2003], where they also studied the high-frequency oscillation (HFO $\sim$ 600 Hz) of very low voltage (<500 nV) accompanying the low frequency N20 component [Curio et al., 1997]. Interestingly, the reported N20 gating was accompanied by attenuation of the late HFO, while the early HFO remained unaffected. Although HFO are generated by different mechanisms than the low frequency component of the N20 [Gobbelé et al., 2004; Urasaki et al., 2006], the comparison with the present β-gamma oscillation sustaining the N30 is difficult because of major methodological differences. In addition to the major difference in frequency band, HFO have been observed and analyzed after the averaging of digitally band-pass filtering (450–750 Hz) of the EEG, and no ERSP and ITC analysis have been performed yet on single trials. In addition, HFO remains temporally limited between the N20 onset and fades before the parietal P27 peak (mean duration of 7 ms) [Nakano and Hashimoto, 1999] and thus occurs early before the more widespread N30 component.

The plausible physiological contribution of β-gamma oscillation phase-locking to the N30 component is reinforced by intracerebral recordings of spontaneous beta rhythm in the pre- and postcentral gyrus and in the frontal medial cortex of humans [Szurhaj et al., 2003, 2005]. Magnetoencephalographic (MEG) studies of the hand sensorimotor areas have showed that finger stimulation induced increment of beta (20–32 Hz) and gamma (36–46 Hz) synchronization. Tecchio et al. [2003, 2004] and Palva et al. [2005] have demonstrated that as early as 30 ms after electrical stimulus given on the finger tip, neural activity phase-locked more strongly and persistently to the consciously perceived stimuli than to the unperceived stimuli. In particular, they reported a phase-locking of the beta (14–28 Hz) and low-gamma (28–40 Hz) oscillation in the contralateral sensori-motor region. Beta EEG oscillations (14–35 Hz) have also been reported in the hand sensory motor area 1 s after termination of a self-paced voluntary movement [Pfurtscheller et al., 1997]. It was previously shown that median nerve stimulation was able to trigger an increase in the power of the 10 and 20 Hz oscillations [Pfurtscheller et al., 1997], but only after a delay of 300 ms, which is ten times later than the occurrence of the present beta oscillation. The same type of stimulation evoked an increase in the power of beta oscillation peaking around 500 ms with a latency onset of 300 ms [Pfurtscheller et al., 2002]. These authors showed a decrease in beta oscillation during hand manipulation whereas the amplitude of P140/N200 SEP components was increased. However, the behavior of early SEP components was not the focus of these studies. In monkeys, field-potential oscillations in the 20–30 Hz range have been reported [Baker et al., 1999] and were supported by synchronous oscillatory activity in a large number of cortical neurons [Murthy and Fetz, 1992] providing synchronization of neuronal firing between somatosensory and motor areas [Wheaton et al., 2005].

It is important to emphasize that the presence of pure phase-locking in resting condition does not exclude that evoked phasic activity occurs when all the trials were taken into account. Indeed, when the trials presenting power enhancement were rejected, we found that the N30 amplitude was significantly decreased. As ITC values remained the same, this amplitude reduction indicates the contribution of phasic activation to the N30 amplitude. As proposed in the case of many ERP components [Basar, 1980], in addition to this phase-resetting effect, the rest of the evoked component may be generated by coherent phasic activation of pyramidal neurons via thalamo-cortical input, as predicted by the additive model.

Resonance in the basal ganglionic-thalamo-cortical loop could be implicated in EEG oscillation triggered by sensory stimulation. Neuronal activity in the 30–80 Hz band is associated with motor function in the presence of normal dopaminergic drive [Brown et al., 2001, 2002; Cassidy et al., 2002; MacKay, 1997] and acts as pacemaker for sensorimotor integration [Humphries et al., 2006]. Although their precise functional role remains an open question, it may provide a temporal window for the processing of sensory information [MacKay, 1997]. This rhythmic activity is replaced by slower oscillations in the off-state of Parkinsonian patients [Brown et al., 2001], and could be related to the N30 alteration in the Parkinsonian off-state [Cheron et al., 1994; Rossini et al., 1993]. Recently, Kühn et al. [2006] suggested that the 30 Hz oscillation in the subthalamic nucleus that is suppressed during finger actual movement or mental imagery in Parkinsonian patients could be physiological and present in normal subjects. In this theoretical framework, the present time frequency behavior of the N30 component could be viewed as resulting from the phase-locking of the basal ganglionic-thalamo-cortical loop activity resonating around 30 Hz. In the absence of movement, this loop may be activated by the sensory stimulation triggering the phase alignment of the 30 Hz EEG oscillation. Conversely, during active movement the loop is involved in movement control and unable to response to the external stimulation.

As described for the auditory 40 Hz oscillation [Ribary et al., 1991], the N30 related beta/gamma rhythm may be viewed as a more global mechanism working in parallel to the stimuli processing of the somatosensory pathway. The phase-locking of this rhythm allows the placement of the sensory signal in the temporal context taking into account the intrinsic functional state of the brain at the arrival time of the stimulus.

Phase resetting of both local field potential and single-unit activity representative of the ongoing motor cortical beta (15–30 Hz) rhythms has been demonstrated in pyramidal tract stimulation in monkeys [Jackson et al., 2002]. This view is also supported by in vitro and in vivo physiological studies [Hughes et al., 2004] showing enhanced oscillation when neurons fire in-phase with the oscillation field. This could explain at a cellular level how the depolarization induced by the sensory stimulus is able to reset the oscillating phase and bring the system into a synchronous attractor basin at the latency of the N30 component. In contrast, during the finger movement the neuronal populations of the sensory motor cortex and other related areas are involved in the ongoing motor cortical beta rhythms assuming the cortico-muscular coherence and the action goals [Baker et al., 1999]. In this active context, it is likely that these neuronal populations could be not responsive to the phasic sensory activation and unable to phase-lock their firing discharges to the external sensory input. Further experimental works will be necessary to dissociate the rhythmic activities linked to motor action from those involved in sensory integration and help to resolve the complex behavior of the N30 component.

CONCLUSION

The important reduction of the frontal N30 occurring throughout its wide topographical extension on the scalp was mainly due to disorganization of the phase-locking of

the beta/gamma EEG oscillations, which normally occurred when the sensory input was not in competition with movement production.

ACKNOWLEDGMENTS

The authors would like to thank Arnaud Delorme and Scott Makeig for their generous gift of software. We wish to thank P. Demaret, M. Dufief, and E. Hortmanns for expert technical assistance.

REFERENCES

Allison T, McCarthy G, Wood CC, Darcey TM, Spencer DD, Williamson PD (1989): Human cortical potentials evoked by stimulation of the median nerve. I. Cytoarchitectonic areas generating short-latency activity J Neurophysiol 62:694–710.

Baker SN, Kilner JM, Pinches EM, Lemon RN (1999): The role of synchrony and oscillations in the motor output. Exp Brain Res 128:109–117.

Barba C, Valeriani M (2004): Assessing somatosensory evoked potential (SEP) generators by human intracranial recordings. Clin Neurophysiol 115:488–489.

Barba C, Frot M, Guénot M, Mauguière F (2001): Stereotactic recordings of median nerve somatosensory-evoked potentials in the human pre-supplementary motor area. Eur J Neurosci 13:347–356.

Barba C, Valeriani M, Restuccia D, Colicchio G, Faraca G, Tonali P, Mauguière F (2003): The human supplementary motor area-proper does not receive direct somatosensory inputs from the periphery: Data from stereotactic depth somatosensory evoked potential recordings. Neurosci Lett 344:161–164.

Barba C, Valeriani M, Colicchio G, Mauguiere F (2005): Short and middle-latency median nerve (MN) SEPs recorded by depth electrodes in human pre-SMA and SMA-proper. Clin Neurophysiol 116:2664–2674.

Basar E (1980): EEG Brain Dynamics: Relation Between EEG and Brain Evoked Potentials. Amsterdam: Elsevier Publisher.

Brown P, Oliviero A, Mazzone P, Insola A, Tonali P, Di Lazzaro V (2001): Dopamine dependency of oscillations between subthalamic nucleus and pallidum in Parkinson's disease. J Neurosci 21:1033–1038.

Brown P, Kupsch A, Magill PJ, Sharott A, Harnack D, Meissner W (2002): Oscillatory local field potentials recorded from the subthalamic nucleus of the alert rat. Exp Neurol 177:581–585.

Buzsáki G, Draguhn A (2004): Neuronal oscillations in cortical networks. Science 304:1926–1929.

Cassidy M, Mazzone P, Oliviero A, Insola A, Tonali P, Di Lazzaro V, Brown P (2002): Movement-related changes in synchronization in the human basal ganglia. Brain 125:1235–1246.

Cheron G (1999): Is the frontal N30 component of the somatosensory evoked potentials a reliable physiological index of the dopaminergic motor pathways? Clin Neurophysiol 110:1698–1699.

Cheron G, Borenstein S (1987): Specific gating of the early somatosensory evoked potentials during active movement. Electroencephalogr Clin Neurophysiol 67:537–548.

Cheron G, Borenstein S (1991): Gating of the early components of the frontal and parietal somatosensory evoked potentials in different sensory-motor interference modalities. Electroencephalogr Clin Neurophysiol 80:522–530.

Cheron G, Borenstein S (1992): Mental movement simulation affects the N30 frontal component of the somatosensory evoked potential. Electroencephalogr Clin Neurophysiol 84:288–292.

Cheron G, Piette T, Thiriaux A, Jacquy J, Godaux E (1994): Somatosensory evoked potentials at rest and during movement in Parkinson's disease: Evidence for a specific apomorphine effect on the frontal N30 wave. Electroencephalogr Clin Neurophysiol 92:491–501.

Cheron G, Dan B, Borenstein S (2000): Sensory and motor interfering influences on somatosensory evoked potentials. J Clin Neurophysiol 17:280–294.

Cheron G, Cebolla AM, De Saedeleer C, Bengoetxea A, Leurs F, Leroy A, Dan B (2007): Pure phase-locking of beta/gamma oscillation contributes to the N30 frontal component of somatosensory evoked potentials. BMC Neurosci 18:8–75.

Cohen LG, Starr A (1987): Localization, timing and specificity of gating of somatosensory evoked potentials during active movement in man. Brain 110:451–467.

Curio G, Mackert BM, Burghoff M, Neumann J, Nolte G, Scherg M, Marx P (1997): Somatotopic source arrangement of 600 Hz oscillatory magnetic fields at the human primary somatosensory hand cortex. Neurosci Lett 234:131–134.

Delorme A, Makeig S (2004): EEGLAB: an open source toolbox for analysis of single-trial EEG dynamics including independent component analysis. J Neurosci Methods 15:9–21.

Desmedt JE, Cheron G (1980): Central somatosensory conduction in man: neural generators and interpeak latencies of the far-field components recorded from neck and right or left scalp and earlobes. Electroencephalogr Clin Neurophysiol 50:382–403.

Desmedt JE, Cheron G (1981): Prevertebral (oesophageal) recording of subcortical somatosensory evoked potentials in man: the spinal P13 component and the dual nature of the spinal generators. Electroencephalogr Clin Neurophysiol 52:257–275.

Durstewitz D, Seamans JK, Sejnowski TJ (2000): Dopamine-mediated stabilization of delay-period activity in a network model of prefrontal cortex. J Neurophysiol 83:1733–1750.

Fukuda C, Tomita Y, Maegaki Y, Kubota N (2003): Frontal N30 of median nerve SSEPs for evaluation of movement disorders with destructive basal ganglia deficits. Neuropediatrics 34:205–210.

Gobbelé R, Waberski TD, Dieckhöfer A, Kawohl W, Klostermann F, Curio G, Buchner H (2003): Patterns of disturbed impulse propagation in multiple sclerosis identified by low and high frequency somatosensory evoked potential components. J Clin Neurophysiol 20:283–90.

Gobbelé R, Waberski TD, Simon H, Peters E, Klostermann F, Curio G, Buchner H (2004): Different origins of low- and high-frequency components (600 Hz) of human somatosensory evoked potentials. Clin Neurophysiol 115:927–937.

Hughes SW, Lorincz M, Cope DW, Blethyn KL, Kekesi KA, Parri HR, Juhasz G, Crunelli V (2004): Synchronized oscillations at alpha and theta frequencies in the lateral geniculate nucleus. Neuron 42:253–268.

Humphries MD, Stewart RD, Gurney KN (2006): A physiologically plausible model of action selection and oscillatory activity in the basal ganglia. J Neurosci 26:12921–12942.

Huttunen J, Hömberg V (1991): Influence of stimulus repetition rate on cortical somatosensory potentials evoked by median nerve stimulation: Implications for generation mechanisms. J Neurol Sci 105:37–43.

Ibañez V, Deiber MP, Mauguière F (1989): Interference of vibrations with input transmission in dorsal horn and cuneate nucleus in man: a study of somatosensory evoked potentials

(SEPs) to electrical stimulation of median nerve and fingers. Exp Brain Res 75:599–610.

Jackson A, Spinks RL, Freeman TC, Wolpert DM, Lemon RN (2002): Rhythm generation in monkey motor cortex explored using pyramidal tract stimulation. J Physiol 541:685–699.

Jansen BH, Agarwal G, Hegde A, Boutros NN (2003): Phase synchronization of the ongoing EEG and auditory EP generation. Clin Neurophysiol 114:79–85.

Jones SJ, Halonen JP, Shawkat F (1989): Centrifugal and centripetal mechanisms involved in the 'gating' of cortical SEPs during movement. Electroencephalogr Clin Neurophysiol 74:36–45.

Kanovsky P, Bares M, Rektor I (2003): The selective gating of the N30 cortical component of the somatosensory evoked potentials of median nerve is different in the mesial and dorsolateral frontal cortex: Evidence from intracerebral recordings. Clin Neurophysiol 114:981–991.

Klimesch W, Sauseng P, Hanslmayr S, Gruber W, Freunberger R (2007): Event-related phase reorganization may explain evoked neural dynamics. Neurosci Biobehav Rev 31:1003–1016.

Kühn AA, Doyle L, Pogosyan A, Yarrow K, Kupsch A, Schneider GH, Hariz MI, Trottenberg T, Brown P (2006): Modulation of beta oscillations in the subthalamic area during motor imagery in Parkinson's disease. Brain 129:695–706.

MacKay WA (1997): Synchonized neuronal oscillations and their role in motor processes. Trends Cogn Sci 1:176–183.

Makeig S, Westerfield M, Jung TP, Enghoff S, Townsend J, Courchesne E, Sejnowski TJ (2002): Dynamic brain sources of visual evoked responses. Science 295:690–694.

Murase N, Kaji R, Shimazu H, Katayama-Hirota M, Ikeda A, Kohara N, Kimura J, Shibasaki H, Rothwell JC (2000): Abnormal premovement gating of somatosensory input in writer's cramp. Brain 123:1813–1829.

Murthy VN, Fetz EE (1992): Coherent 25- to 35-Hz oscillations in the sensorimotor cortex of awake behaving monkeys. Proc Natl Acad Sci USA 89:5670–5674.

Nakano S, Hashimoto I (1999): The later part of high-frequency oscillations in human somatosensory evoked potentials is enhanced in aged subjects. Neurosci Lett 276:83–86.

O'Reilly RC (2006): Biologically based computational models of high-level cognition. Science 314:91–94.

Palva S, Linkenkaer-Hansen K, Näätänen R, Palva JM (2005): Early neural correlates of conscious somatosensory perception. J Neurosci 25:5248–5258.

Pfurtscheller G, Stancak A Jr, Edlinger G (1997): On the existence of different types of central beta rhythms below 30 Hz. Electroenceph Clin Neurophysiol 102:316–325.

Pfurtscheller G, Woertz M, Muller G (2002): Wriessnegger S, Pfurtscheller K. Contrasting behavior of beta event-related synchronization and somatosensory evoked potential after median nerve stimulation during finger manipulation in man. Neurosci Lett 323:113–116.

Pierantozzi M, Mazzone P, Bassi A, Rossini PM, Peppe A, Altibrandi MG, Stefani A, Bernardi G, Stanzione P (1999): The effect of deep brain stimulation on the frontal N30 component of somatosensory evoked potentials in advanced Parkinson's disease patients. Clin Neurophysiol 110:1700–1007.

Press WH, Flannery BP, Teukolsky SA, Vettering WT (1992): Numerical Recipes in C, 2nd ed. Cambridge: Cambridge University Press.

Ribary U, Ioannides AA, Singh KD, Hasson R, Bolton JP, Lado F, Mogilner A, Llinás R (1991): Magnetic field tomography of coherent thalamocortical 40-Hz oscillations in humans. Proc Natl Acad Sci USA 88:11037–11041.

Rossi S, Tecchio F, Pasqualetti P, Ulivelli M, Pizzella V, Romani GL, Passero S, Battistini N, Rossini PM (2002): Somatosensory processing during movement observation in humans. Clin Neurophysiol 113:16–24.

Rossini PM, Paradiso C, Zarola F, Bernardi G, Caramia MD, Margari L, Ferrari E (1991): Brain excitability and long latency muscular arm responses: Non-invasive evaluation in healthy and parkinsonian subjects. Electroencephalogr Clin Neurophysiol 81:454–65.

Rossini PM, Traversa MD, Boccasena MD, Martino G, Passarelli F, Pacifici L, Bernardi G, Stanzione P (1993): Parkinson's disease and somatosensory evoked potentials: Apomorphine-induced transient potentiation of frontal components. Neurology 43:495–500.

Rossini PM, Bassetti MA, Pasqualetti P (1995): Median nerve somatosensory evoked potentials. Apomorphine-induced transient potentiation of frontal components in Parkinson's disease and in parkinsonism. Electroencephalogr Clin Neurophysiol 96:236–247.

Rossini PM, Babiloni C, Babiloni F, Ambrosini A, Onorati P, Carducci F, Urbano A (1999): 'Gating' of human short-latency somatosensory evoked cortical responses during execution of movement. A high resolution electroencephalography study. Brain Res 843:161–170.

Roland PE, Larsen B, Lassen NA, Skinhøj E (1980): Supplementary motor area and other cortical areas in organization of voluntary movements in man. J Neurophysiol 43:118–36.

Rushton DN, Rothwell JC, Craggs MD (1981): Gating of somatosensory evoked potentials during different kind of movement in man. Brain 104:465–491.

Sauseng P, Klimesch W, Gruber WR, Hanslmayr S, Freunberger R, Doppelmayr M (2007): Are event-related potential components generated by phase resetting of brain oscillations? A critical discussion. Neuroscience 146:1435–1444.

Shah AS, Bressler SL, Knuth KH, Ding M, Mehta AD, Ulbert I, Schroeder CE (2004): Neural dynamics and the fundamental mechanisms of event-related brain potentials. Cereb Cortex 14:476–483.

Singer W (1999): Neuronal synchrony: A versatile code for the definition of relations? Neuron 24:49–65,111–125.

Sober SJ, Sabes PN (2005): Flexible strategies for sensory integration during motor planning. Nat Neurosci 8:490–497.

Steriade M (2001): Impact of network activities on neuronal properties in corticothalamic systems. J Neurophysiol 86:1–39.

Steriade M, Jones EG, McCormick DA (1997): Thalamus, Organization and Function. Amsterdam: Elsevier.

Szurhaj W, Derambure P, Labyt E, Cassim F, Bourriez JL, Isnard J, Guieu JD, Mauguiere F (2003): Basic mechanisms of central rhythms reactivity to preparation and execution of a voluntary movement: A stereoelectroencephalographic study. Clin Neurophysiol 114:107–119.

Szurhaj W, Bourriez JL, Kahane P, Chauvel P, Mauguière F, Derambure P (2005): Intracerebral study of gamma rhythm reactivity in the sensorimotor cortex. Eur J Neurosci 21:1223–1235.

Tallon-Baudry C, Bertrand O, Delpuech C, Pernier J (1996): Stimulus specificity of phase-locked and non-phase-locked 40 Hz visual responses in human. J Neurosci 16:4240–4249.

Tecchio F, Babiloni C, Zappasodi F, Vecchio F, Pizzella V, Romani GL, Rossini PM (2003): Gamma synchronization in human primary somatosensory cortex as revealed by somatosensory evoked neuromagnetic fields. Brain Res 986:63–70.

Tecchio F, De Lucia M, Salustri C, Montuori M, Bottaccio M, Babiloni C, Pietronero L, Zappasodi F, Rossini PM (2004): District-related frequency specificity in hand cortical representation: Dynamics of regional activation and intra-regional synchronization. Brain Res 1014:80–86.

Tinazzi M, Valeriani M, Moretto G, Rosso T, Nicolato A, Fiaschi A, Aglioti SM (2004): Plastic interactions between hand and face cortical representations in patients with trigeminal neuralgia: A somatosensory-evoked potentials study. Neuroscience 127:769–776.

Urasaki E, Genmoto T, Yokota A, Maeda R, Akamatsu N (2006): Effects of general anesthesia on high-frequency oscillations in somatosensory evoked potentials. J Clin Neurophysiol 23:426–430.

Urushihara R, Murase N, Rothwell JC, Harada M, Hosono Y, Asanuma K, Shimazu H, Nakamura K, Chikahisa S, Kitaoka K, Sei H, Morita Y, Kaji R (2006): Effect of repetitive transcranial magnetic stimulation applied over the premotor cortex on somatosensory-evoked potentials and regional cerebral blood flow. Neuroimage 31:699–709.

Yeung N, Bogacz R, Holroyd CB, Cohen JD (2004): Detection of synchronized oscillations in the electroencephalogram: An evaluation of methods. Psychophysiology 41: 822–832.

Wheaton LA, Nolte G, Bohlhalter S, Fridman E, Hallett M (2005): Synchronization of parietal and premotor areas during preparation and execution of praxis hand movements. Clin Neurophysiol 116:1382–1390.